Photoluminescence of a Freely Suspended Monolayer of Quantum Dots Encapsulated into Layer-by-Layer Films

Dmitry Zimnitsky,[†] Chaoyang Jiang,[†] Jun Xu,[‡] Zhiqun Lin,[‡] Lei Zhang,[§] and Vladimir V. Tsukruk*,[†]

School of Materials Science and Engineering, Georgia Institute of Technology, Atlanta, Georgia 30332, Department of Materials Science and Engineering, Iowa State University, Ames, Iowa 50011, and Agiltron Incorporated, Woburn, Massachusetts 01801

Received May 18, 2007. In Final Form: July 13, 2007

A single monolayer of CdSe/ZnS quantum dots (QDs) has been encapsulated into a 60 nm free-suspended layer-by-layer (LbL) film. The QD monolayer showed a low light-emission within this film in contact with supporting solid substrates, but the manifold increase of photoluminescencence intensity was observed when the film was lifted and freely suspended over the microfabricated cylindrical cavities. This phenomenon was discussed in relationship with the effect of the elimination of the surface quenching enhanced by optical reflection from highly reflective silicon cavities. We suggest that a significant increase of the photoluminescence intensity of QD monolayers suspended over the microfabricated array can be interesting for future diagnostic and sensing applications.

Introduction

Nanocrystals of II−VI semiconductors (e.g., CdS, CdSe, and CdTe) prepared as colloids in the 1−10 nm size range have generated tremendous interest over the past decade in physics, chemistry, and engineering due to their unique optical and electronic properties.[1] These nanocrystals are prototypical quantum dots (QDs) with their optical properties governed by quantum mechanics. The good photostability, high photoluminescence (PL) intensity, and wide emission tunability make QDs an excellent choice as novel chromophores. In comparison with organic dyes, this class of luminescent labels have high quantum yield, high molar extinction coefficients (10−100 times higher than that of organic dyes),[2,3] and narrow, symmetric PL bands (full-width at half-maximum within 25−40 nm), spanning from UV to near-infrared range.[4] These properties along with resistance to photobleaching can be very useful in the development of sensitive detection routines for DNA sequencing, clinical diagnostics, and fundamental molecular biological studies. Processing of QDs in combination with polymeric materials may allow fabrication of flexible luminescent materials in the form of films, fibers, and 3D structures. Several reports devoted to the controlled incorporation of QDs in a polymeric matrix resulting in nanocomposites with controllable light-emission can be found in the literature.[5−7]

One of the more successful approaches employed was layer-by-layer (LbL) assembly which allows controlled placement of charged nanoparticles such as QDs between polymeric multilayers.[8,9−12] Kotov et al.[13] and Oliveira and co-workers[14] have fabricated multilayered composites with alternating layers of polycation and semiconductor nanoparticles. A linear dependence of UV−vis absorption and emission upon the number of nanoparticles layers confirmed the regular deposition of the polyelectrolytes and QDs. The importance of the host polymer matrix in the LbL films was demonstrated by the observation that the PL intensity of PAMAM (poly(amidoamine))/CdSe films is ca. 50 times higher than the PL from PAH/CdSe films. In another study, Leblanc et al. prepared a combined LbL film containing several bilayers of chitosan and CdSe QDs, covered with two bilayers of organophosphorus hydrolase/QDs.[15] They showed that sandwiching QDs within the LbL film enhances the PL intensity compared with QD solution presumably due to a higher degree of surface passivation that improves the electron−hole recombination process.

The formation of QD monolayers has been studied on different polycations, (3-aminopropyl)-triethoxysilane (APTES), polyethylenimine (PEI), and poly(diallydimethylammonium) chloride (PDDA).[16] The marked difference in the structural characteristics of the QD layers such as overall particle density and distribution has been found. On the PDDA-coated surface, QDs are adsorbed in a homogeneous close-packed monolayer with little aggregation or multilayer formation. Unlike PDDA, significant aggregation of QDs occurs on PEI or the APTES-modified surface, and the clusters of single QD are seen. In another study, the possibility of preparation of a graded semiconductor film on the base of QDs with different sizes and PDDA has been reported. The graded

* To whom correspondence should be addressed. E-mail: vladimir@mse.gatech.edu.
[†] Georgia Institute of Technology.
[‡] Iowa State University.
[§] Agiltron Incorporated.

(1) Cordero, S. R.; Carson, P. J.; Estabrook, R. A.; Strouse, G. F.; Buratto, S. K. *J. Phys. Chem. B* **2000**, *104*, 12137.
(2) Medintz, I. L.; Uyeda, H. T.; Goldman, E. R.; Mattousi, H. *Nat. Mater.* **2005**, *4*, 435.
(3) Leatherdale, C. A.; Woo, W.-K.; Mikulec, F. V.; Bawendi, M. G. *J. Phys. Chem. B* **2002**, *106*, 7619.
(4) Warren, C. W.; Nie, S. *Science* **1998**, *281*, 5385.
(5) Bol, A. A.; Meijerink, A. *J. Phys. Chem. B* **2001**, *105*, 10203.
(6) Wang, C.-W.; Moffitt, M. G. *Langmuir* **2004**, *20*, 11784.
(7) Shavel, A.; Gaponik, N.; Eychmüller, A. *Eur. J. Inorg. Chem.* **2005**, *18*, 3613.
(8) Jiang, C.; Markutsya, S.; Pikus, Y.; Tsukruk, V. V. *Nat. Mater.* **2004**, *3*, 721.
(9) Jiang, C.; Tsukruk, V. V. *Adv. Mater.* **2006**, *18*, 829.
(10) *Multilayer Thin Films*; Decher, G., Schlenoff, J. B., Eds.; Wiley-VCH: Weinheim, Germany, 2003.
(11) *Protein Architecture: Interfacial Molecular Assembly and Immobilization Biotechnology*; Lvov, Y., Möhwald, H., Eds.; Marcel Dekker: New York, 2000.
(12) Tang, Z.; Kotov, N. A. *Adv. Mater.* **2005**, *17*, 951.
(13) Kotov, N. A.; Dekany, I.; Fendler, J. H. *J. Phys. Chem.* **1995**, *99*, 13065.
(14) Zucolotto, V.; Gatta's-Asfura, K. M.; Tumolo, T.; Perinotto, A. C.; Antunes, P. A.; Constantino, C. J. L.; Baptista, M. S.; Leblanc, R. M.; Oliveira, O. N., Jr. *Appl. Surf. Sci.* **2005**, *246*, 397.
(15) Constantine, C. A.; Gatta's-Asfura, K. M.; Mello, S. V.; Crespo, G.; Rastogi, V.; Cheng, T.-C.; DeFrank, J. J.; Leblanc, R. M. *J. Phys. Chem. B* **2003**, *107*, 13762.
(16) Tang, Z.; Wang, Y.; Kotov, N. A. *Langmuir* **2002**, *18*, 7035.

10.1021/la7014644 CCC: $37.00
Published on Web 08/29/2007

multilayer QD films were assembled by using four different CdTe dispersions, which display respectively green, yellow, orange, and red luminescence.[17] Murase and co-workers used the LbL method for the preparation of QD multilayers with high PL intensity.[18] They exploited functionalized aminosilane glass as a substrate and thioglycolic acid or mercaptosilanes as linkers to obtain different color-light-emitting films with many layers of QDs. On the other hand, covalent linking of conjugated polymers was required to create bright multilayered LbL films with interesting photovoltaic properties.[19] Otherwise, the QDs have been incorporated into bulk polymeric materials which are incompatible with microfabricated devices and have low mechanical strength.[20] Light emitting diodes based on the stack of multiple layers of QDs and conjugated polymer poly(*p*-phenylene vinylene) (PPV) has been constructed.[21] The combination of CdSe nanoparticles and PPV was beneficial for both of them regarding the stability of the electroluminescence.

All aforementioned QD-containing luminescent materials have been prepared in the form of molecular films supported by bulk substrates, usually glass or silicon. Their overall uniformity, integrity, and robustness frequently remain uncovered. The close proximity to the solid surface (especially metal substrates) can easily result in significant quenching of luminescence as indeed has been observed on many occasions for organic chromophores.[22,23] As have been observed, placing molecularly thin films with QDs on a metal or semiconducting substrate can cause significant quenching of the PL intensity which can be worsened by microroughness of the substrate, which further inhibits the reflective intensity.[24] To obtain even modest PL intensity from QDs arrays, the researchers usually deposit several layers of nanoparticles effectively increasing their volume content compromising on film quality, thickness, and uniformity.

The application of luminescent films as a sensing part of flexible, organo-electronic devices requires robust albeit flexible, easily transferable, and highly luminescent QD-containing films. Our group previously demonstrated the possibility of the facile fabrication of robust ultrathin free-standing films with encapsulated nanoparticles of different types.[8,9] However, these films contained gold nanoparticles and carbon nanotubes for reinforcement and had little or no optical activity. Here, we demonstrate that the incorporation of QDs into ultrathin (tens of a nanometer) polymeric films provides robust nanoscale films with tunable light-emitting properties. These films with a thickness as small as 60 nm are flexible enough to be transferred on various substrates (silicon, poly dimethyl siloxane (PDMS), copper grid, quartz, and glass). The QD-containing films can be freely suspended over microscopic openings in these substrates and sustain significant stresses during the drying procedure and variable hydrostatic air pressure. Moreover, LbL-QD films suspended over optical cavities microfabricated in a silicon wafer demonstrated dramatically increased light-emission as compared to the same QD film in physical contact with a silicon surface due to the enhanced optical backlight reflection and the elimination of substrate quenching. Unlike previous studies which rely either on LbL films with many layers of QDs or bulk polymers with a high concentration of QD to create polymeric structures with bright fluorescence, this research demonstrates a true monolayer of QDs with relatively low nanoparticle density, which is "packaged" into nanoscale flexible films providing controllable PL response, easy handling, and transfer to any microfabricated array.

Experimental Section

Materials. The polyelectrolytes, poly(allylamine hydrochloride) (PAH), MW = 70 000), and poly(sodium 4-styrenesulfonate) (PSS), MW = 70 000) were purchased from Aldrich and used without further purification. Ultrapure water with a resistivity $\sigma > 18.0$ MΩ cm used in all experiments was purified with a Nanopure system. Silicon wafers and quartz substrates were cut to a typical size of 10 × 20 mm and were cleaned in a piranha solution [1:3 (v/v) H_2SO_4/H_2O_2], according to a usual procedure adapted in our laboratory.[25] Attention: piranha solution is extremely dangerous and should be handled very carefully. Silicon wafers of the {100} orientation with one side polished (Semiconductor Processing Co.) and quartz plates with both sides polished (Chemglass Co.) were atomically smooth (microroughness within 1 × 1 μm surface area below 0.1 nm). After cleaning, the substrates were rinsed thoroughly with Nanopure water and dried with dry nitrogen before they were used. A PDMS substrate with and without circle-shaped cavities (diameter 20 μm, depth 50 μm) were prepared by curing liquid pre-polymer (Sylgard 184, Dow Chemical) on top of the corresponding silicon template at room temperature overnight under vacuum. The microfabricated silicon wafers with microcavity arrays were prepared as described elsewhere. Briefly, the half-inch, 64 × 64 array of microcavities with the 80 μm diameter and the 70 μm depth were fabricated by etching the cylindrical holes using the deep reactive ion etching processing.[26,27]

Synthesis of CdSe Nanoparticles. Core−shell CdSe/ZnS QDs were prepared according to the known procedure.[28,29] An amount of ZnS precursor [diethylzinc ($Zn(CH_2CH_3)_2$):hexamethyl(disilathiane) ($(TMS)_2S$) = 1:1 in trioctylphosphine (TOP)] were added in tri-*n*-octylphosphine oxide (TOPO)-functionalized CdSe solution at elevated temperature. The resulting organic soluble CdSe/ZnS QDs were subsequently converted into water soluble nanoparticles via ligand exchange with thioacetic acid (TAA) according the usual procedure.[30] In brief, TOP-capped CdSe−ZnS QDs were dissolved in a 1 M solution of TAA in dichloromethane. The mixture was stirred vigorously overnight followed by injection of slightly basic water (pH 8) for extraction of TAA-coated QDs into the water phase. To remove the exccess TAA, the aqueous QD solution was centrifuged at 15 000 rpm, washed, and redispersed in basic water. The concentration of QDs solution was calculated from amount from precursor taken for QDs synthesis.

Fabrication of Freely Suspended Membranes. A sacrificial cellulose acetate (CA) layer was spin cast on the freshly cleaned silicon substrate.[8,9,31] A droplet (150 μL) of 2 wt % CA acetone solution containing 1 wt % water was placed on the silicon substrate and rotated for 20 s with a 3000 rpm. The multilayer LbL-QD polymer films (general formula: (PAH/PSS)nPAH/QD/(PAH/PSS)n/PAH)) were fabricated using LbL method as discussed in detail earlier.[32,33,34,35,36]On top of CA a layer of PAH was deposited from 0.2w% PAH solution by spin-casting for 20 s with a 3000 rpm. The substrate was rinsed twice with Nanopure water and dried while spinning for 20 s. In the same manner, 0.2% PSS solution was deposited. This procedure was repeated until the needed number of polymer bilayers, *n*, was achieved. To form the central layer, a 150 μL droplet of CdSe/ZnS QD solution was dropped on the substrate

(17) Mamedov, A. A.; Belov, A.; Giersig, M.; Mamedova, N. N.; Kotov, N. A. *J. Am. Chem. Soc.* **2001**, *123*, 7738.
(18) Yang, P.; Li, C. L.; Murase, N. *Langmuir* **2005**, *21*, 8913.
(19) Liang, Z.; Dzienis, K. L.; Wang, Q. *Adv. Funct. Mater.* **2006**, *16*, 542.
(20) Esteves, A. C.; Barros-Timmons, A.; Monteiro, T.; Trindade, T. *J. Nanosci. Nanotechnol.* **2005**, *5*, 766.
(21) Gao, M.; Lesser, C.; Kirstein, S.; Mohwald, H.; Rogach, A. L.; Weller, H. *J. Appl. Phys.* **2000**, *87*, 2297.
(22) Chance, R. R.; Prock, A.; Silbey, R. *Adv. Chem. Phys.* **1978**, *37*, 1.
(23) Singamaneni, S.; Jiang, C.; Merrick, E.; Kommireddy, D.; Tsukruk, V. V. *J. Macromol. Sci. Part B: Phys.* **2007**, *46*, 1.
(24) Pacifico, J.; Jasieniak, J.; Gomez, D.; Mulvaney, P. *Small* **2006**, *2*, 199.
(25) Tsukruk, V. V.; Bliznyuk, V. N. *Langmuir* **1998**, *14*, 446.
(26) Yan, D.; Cheng, J.; Apsel, A. *Sens. Actuators, A* **2004**, *115*, 60.
(27) Yan, D.; Apsel, A.; Lal, A. *Smart Mater. Struct.* **2005**, *14*, 775.
(28) Peng, X.; Manna, L.; Yang, W. D.; Wickham, J.; Scher, E.; Kadavanich, C.; Alivisatos, A. P. *Nature* **2000**, *404*, 59.
(29) Xu, J.; Xia, J.; Wang, J.; Shinar, J.; Lin, Z. *Appl. Phys. Lett.* **2006**, *89*, 133110.
(30) Chan, W. C. W.; Nie, S. *Science* **1998**, *281*, 2016.
(31) Jiang, C.; Markutsya, S.; Shulha, H.; Tsukruk, V. V. *Adv. Mater.* **2005**, *17*, 1669.

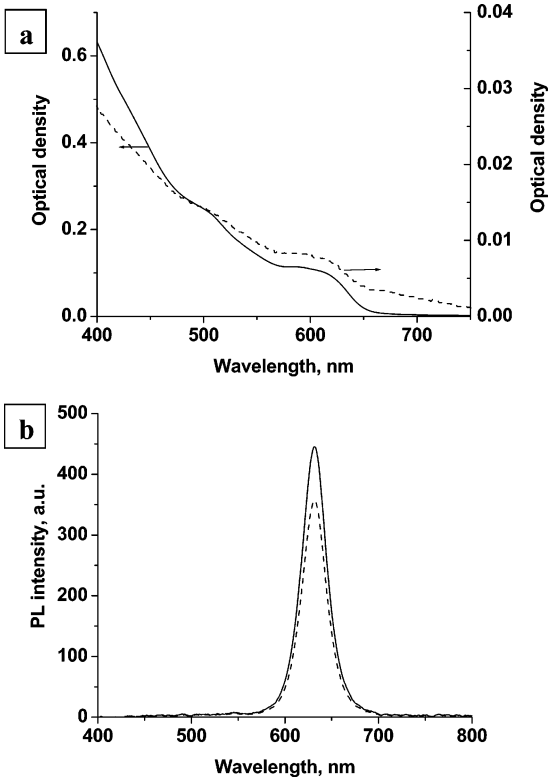

Figure 1. Solid line: absorption (a) and luminescence (b) spectra of 0.1 wt % QD solution. Dashed line: spectra of QD cast monolayer on a quartz surface.

and rotated for 20 s with a 3000 rpm. The substrate was then rinsed twice with Nanopure water and the same number of polymer bilayers, *n*, was again deposited.

For the estimation of the surface density of QDs, two LbL bilayers were deposited first and QDs were deposited subsequently using solutions with different concentrations. The QDs were covered with an additional PAH monolayer to stabilize the surface before AFM scanning. To visualize individual QD nanoparticles and to estimate their size distribution, we deposited a QD monolayer from a very diluted solution (0.01 wt %) on a silicon wafer covered with a monolayer of PAH.

All procedures were performed in Cleanroom class 100. Finally, the LbL films were cut into approximately 2×2 mm^2 squares using a stainless steel microneedle. They were then released by submersion in acetone, which dissolves the CA layer.[37] The LbL films were next transferred to Nanopure water where they could be picked up with various substrates.

Instrumentation. UV−vis spectra were recorded with UV-1601 spectrometer (Shimadzu). AFM images were collected using a Dimension 3000 AFM microscope (Digital Instruments) in the tapping mode according to the usual procedure adapted in our laboratory for ultrathin polymer films.[38] AFM images were obtained with scan sizes ranging from 1 to 10 μm. To obtain a film thickness, the LbL film was picked up on the silicon wafer and the film edge was scanned by AFM. Transmission electron microscopy (TEM) was done using a JEOL 1200EX electron microscope operated at 80 kV. Bright field optical and fluorescent images were captured with an optical fluorescent microscope Leica

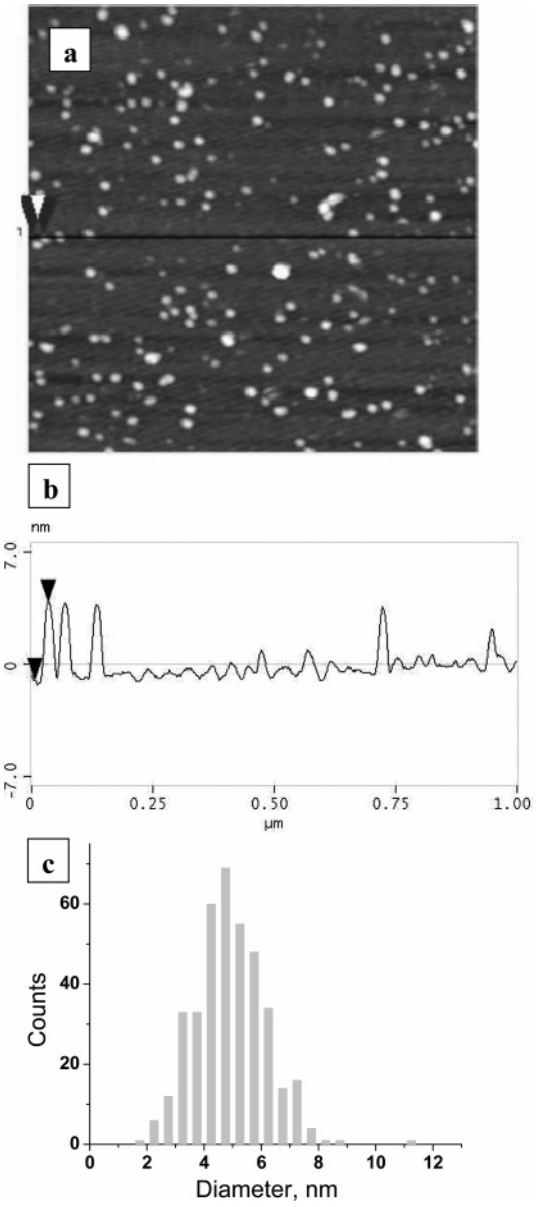

Figure 2. (a) AFM image of QDs adsorbed on the PAH layer from 0.01% QD solution. The *z* scale is 15 nm. (b) Cross-section of CdSe QDs collected along solid line in part a. (c) QD height distribution derived from the AFM cross-sectional data.

DM4000M (an excitation wavelength at 365 nm). Luminescence spectra of the LbL-QD films were recorded using a Craig QDI 202 point-shot spectrophotometer attached to the microscope (fluorescence excitation 365 nm, sampling area 1×1 μm, collection time 15 s).

Buckling Test. The buckling test was conducted for the evaluation of the elastic modulus of LbL films in accordance with the usual procedure.[39,40] For an isotropic film, a uniform buckling pattern having a characteristic wavelength, λ, takes place when it is subjected above a critical compressive stress, and this spacing can be used to evaluate the elastic modulus.[41] To initiate the buckling pattern, a 2×2 mm LbL-QD film was placed over a 0.6×0.6 cm $\times$ 0.4 cm PDMS substrate which was slowly compressed with a micronsized increment. The total compressive distance was generally less than 15 μm keeping compressive strain below 2%. The compression was monitored in a differential interference contrast (DIC) mode adjusted

(32) Jiang, C.; Markutsya, S.; Tsukruk, V. V. *Adv. Mater.* **2004**, *16*, 157.
(33) Jiang, C.; Singamaneni, S.; Merrick, E.; Tsukruk, V. V. *Nano Lett.* **2006**, *6*, 2254.
(34) Lvov, Y.; Decher, G.; Möhwald, H. *Langmuir* **1993**, *9*, 481.
(35) Decher, G. *Science* **1997**, *277*, 1232.
(36) Tang, Z.; Kotov, N. A.; Magonov, S.; Ozturk, B. *Nat. Mater.* **2003**, *2*, 413.
(37) Mamedov, A. A.; Kotov, N. A. *Langmuir* **2000**, *16*, 5530.
(38) Luzinov, I.; Julthongpiput, D.; Tsukruk, V. V. *Macromolecules* **2000**, *33*, 7629.
(39) Xiong, Y.; Xie, Y.; Wu, C.; Yang, J.; Li, Z.; Xu, F. *Adv. Mater.* **2003**, *15*, 405.
(40) Sun, X.; Li, Y. *Adv. Mater.* **2005**, *17*, 2626.
(41) Park, J.-H.; Oh, S.-G.; Jo, B.-W. *Mater. Chem. Phys.* **2004**, *87*, 301.

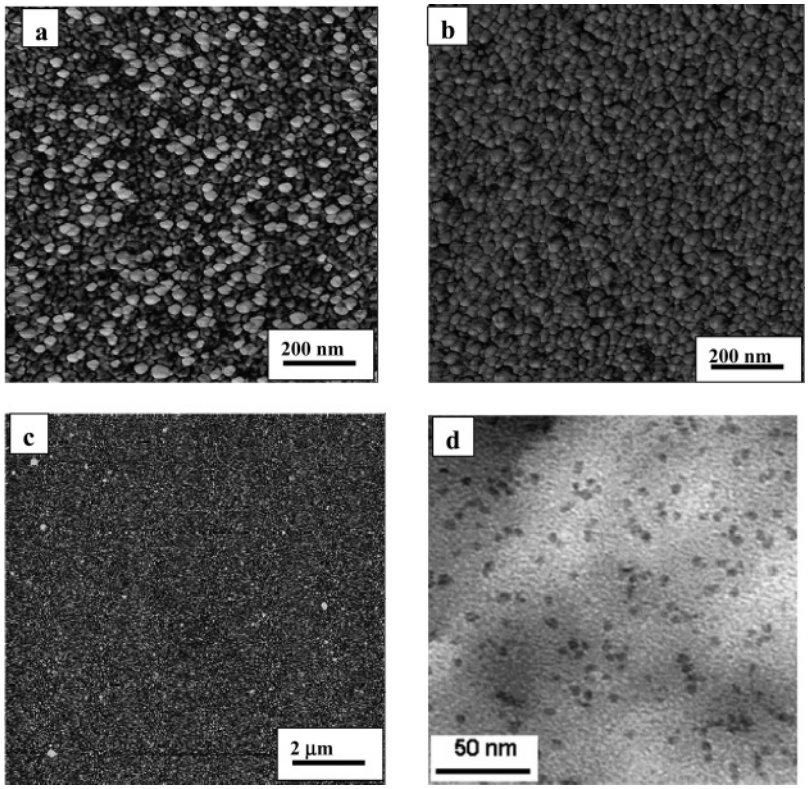

Figure 3. (a, b) AFM phase images of LbL films with general formula $(PAH/PSS)_2PAH/QD/PAH$. The *z* scale is 40°. Central QD layer was deposited using 0.017% (a) and 0.1% (b) solutions. (c) large area AFM topographical image of the film (b). The *z* scale is 20 nm. (d) TEM image of $(PAH/PSS)_9PAH/QD/(PAH/PSS)_9/PAH$ free-standing film. QD layer was deposited using 0.1% QD solution.

for maximum contrast. The digital images were analyzed by using Fourier transformation within ImageJ software.

Results and Discussion

QD Properties in Solution and on the Polyelectrolyte Surface. QDs deposited on a quartz substrate showed an adsorption maximum at 590 nm and a less pronounced peak at 490 nm (Figure 1a).[42] The corresponding light-emission can be observed as a pronounced and narrow PL peak at 633 nm, which is common for CdSe QDs with about 5 nm diameter (Figure 1b).[2] Full width at half-maximum of the PL peak at 30 nm is within the range usually observed for these QDs in a solution.[4]

Figure 2a shows surface morphology of QDs adsorbed from solution on a silicon wafer covered with a monolayer of PAH. Deposition of QDs was made from a diluted (0.01%) solution to visualize individual QDs and estimate nanoparticles size distribution from cross-sectional analysis (Figure 2b,c). Although lateral dimensions of nanoparticles appear to be larger on AFM images than they actually are due to the dilation effect, the height of spherical nanoparticles is a reliable proof of their size.[43,44] The height histogram calculated from the AFM image shows a relatively narrow distribution with the average height at 4.9 ± 1.2 nm which is close to that obtained from TEM data 4.5 ± 0.5 nm (see below). This difference is caused by the presence of the thin organic shell not visible in TEM. On the other hand, the position of the UV−vis absorption peak corresponds to a CdSe nanoparticle diameter of 4.3 nm as can be derived from plots suggested in refs 45 and 46. The difference in the apparent diameters estimated from UV−vis spectroscopy and AFM can be referred to the additional contribution of the ZnS capping layer.

Different Surface Density of QDs on the PAH Surface. To analyze the surface distribution of QDs deposited on the PAH surface, we prepared three different films with QDs deposited from solutions with different concentrations as described in the Experimental Section. High-resolution AFM images show predominantly individual nanoparticles and their small aggregates (with lateral dimensions significantly dilated due to the convolution with the AFM tip end; Figure 3). The surface density of QDs increases with the increase of the concentration of QD solution used for the particle deposition (Figure 3a,b). Even for the highest density of packing, the surface coverage is scarce as illustrated by the TEM image (Figure 3d). Moreover, even for the highest surface density tested here, a relatively uniform distribution of nanoparticles is observed and no signs of the formation of the second layer of QD nanoparticles or larger aggregates on the PAH surface (Figure 3c). This behavior is very different from highly aggregated state observed for CdSe nanoparticles adsorbed on branched polymer layers and SAMs but similar to those observed for other polyelectrolyte surfaces.

For unambiguous evaluation of the actual surface coverage with QDs, we applied a different approach which is not biased by the AFM tip dilation effect.[47] In this approach, a number of QD nanoparticles were directly calculated for each concentration from AFM (if it was possible) and TEM images. The actual surface coverage was evaluated from the number of nanoparticles per unit of surface area and their average diameter. Following

(42) Andreev, A. D.; Datsiev, R. M.; Seisyan, R. P. *Phys. Status Solidi B* **1999**, *215*, 325.
(43) Tsukruk, V. V. *Rubber Chem. Technol.* **1997**, *70*, 430.
(44) Tsukruk, V. V.; Reneker, D. H. *Polymer* **1995**, *36*, 1791.
(45) Murray, C. B.; Norris, D. J.; Bawendi, M. G. *J. Am. Chem. Soc.* **1993**, *115*, 8706.
(46) Yu, W. W.; Qu, L.; Guo, W.; Peng, X. *Chem. Mater.* **2003**, *15*, 2854.
(47) Jiang, C.; Markutsya, S.; Tsukruk, V. V. *Langmuir* **2004**, *20*, 882.

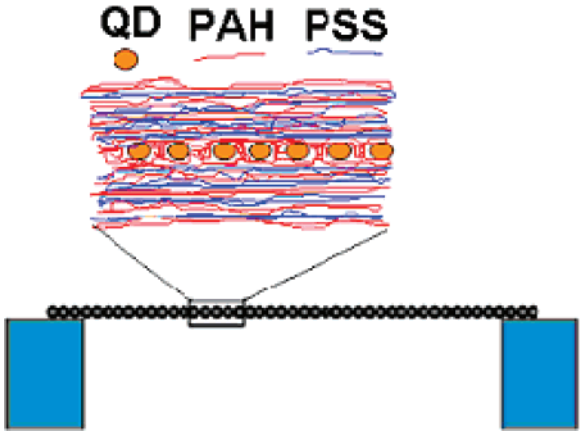

Figure 4. General schematic of the freely suspended LbL film and the microstructure of the LbL film with encapsulated QD nanoparticles, $(PAH/PSS)_9PAH/QD/(PAH/PSS)_9/PAH$.

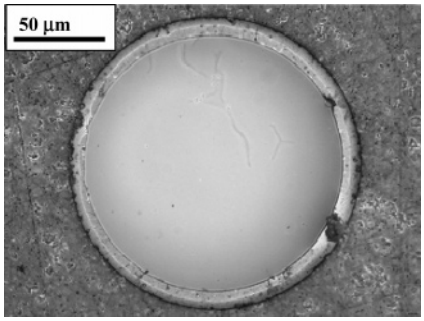

Figure 5. Bright-field image of the free-standing QD LbL film picked up on a copper plate with a 150 μm diameter hole.

this routine, we estimated a number of adsorbed nanoparticles increasing from 200 to 3000 particles per μm^2 at adsorption conditions exploited here. Therefore, the highest surface coverage achieved in this study was 6%, which is much lower than the surface coverage achieved for larger gold nanoparticles covered with a citrate layer (13 nm diameter) in our previous work.[32] However, the surface coverage employed here is significantly higher than those reported in previous studies on CdSe/ZnS QD adsorption on the polyelectrolyte surface. The possible reason for low surface density is the presence of hydrophobic TOP molecules at the QD surface due to incomplete exchange of TOP for TGA. It can cause the aggregation of particles in the solution as well as reduce the surface charge of nanoparticles.

Free-Standing LbL Films with Different Contents of QDs. A general schematic of freely suspended LbL films with encapsulated central monolayer of QD nanoparticles fabricated in this work is shown in Figure 4. Overall, we have fabricated three free-standing LbL-QD films with a general formula $(PAH/PSS)_9PAH/QD/(PAH/PSS)_9/PAH$ (or briefly 9QD9) with different densities of central QD monolayer by using solutions with different QD concentrations (0.017, 0.033, and 0.1%) as described in the Experimental Section.

The thickness of QD-containing films varied between 55 and 60 nm with a general trend to an increase with the increasing QD surface density. LbL films with different volume fractions of QD nanoparticles fabricated here were stable and robust in acetone solution, thus allowing their successful transfer to different solid substrates and suspension across the microscopic openings. An example of an optical image of the free-standing LbL-QD film picked up on a copper plate with a hole shown in Figure 5 demonstrates its integrity despite high residual stresses

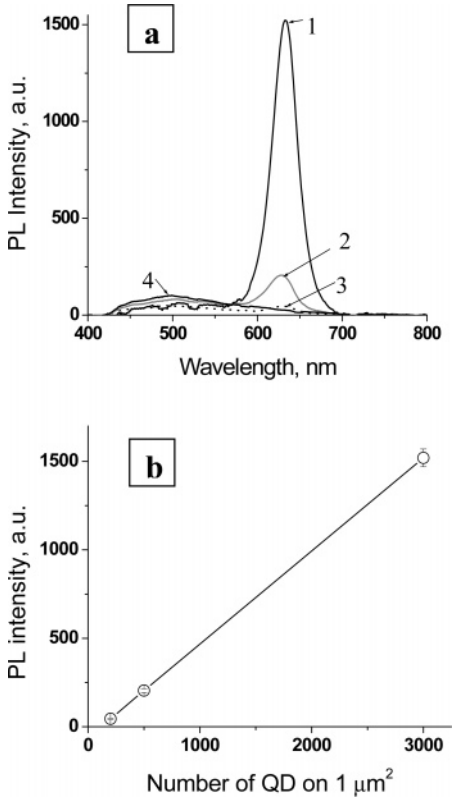

Figure 6. (a) PL spectra of 9QD9 films on the silicon surface. Central QD layer was deposited using solutions with different QD concentrations: 0.1% (1), 0.033% (2), and 0.017% (3). (4) substrate background. (b) Dependence of PL intensity at 633 nm upon the surface density of QD nanoparticles.

developed in the course of this transfer and drying as was revealed in our previous studies for the freely suspended LbL films.[33]

Micromechanical behavior of LbL-QD films was studied using a buckling instability test described in detail in our previous papers.[48] The results confirmed their excellent mechanical properties with the ability to sustain high mechanical stresses. The Young's modulus was estimated from the buckling periodicity in accordance with the known approach.[49,50] The polymeric LbL films without QDs showed modulus 1.4 GPa indicating the mechanical stiffness common for glassy polymers and close to that determined earlier for PAH-PSS LbL films.[51] The value of the elastic modulus increased slightly with incorporation of QDs (1.4−2.0 GPa depending on QD content) but overall was close to those values measured earlier for PSS-PAH LbL films. Thus, unlike previous examples of gold nanoparticles and carbon nanotubes, which provided strong filler reinforcement,[52] we observed an insignificant increase of overall strength of the films. This difference can be related to a very low volume content of QD nanoparticles (within 0.02−0.3 vol %).

Photoluminescence Properties of LbL-QD Films. All LbL films fabricated here showed a single luminescent peak with the parameters identical to those obtained for QD solution and cast layer indicating that full encapsulation of QDs into LbL films

(48) Markutsya, S.; Jiang, C.; Pikus, Y.; Tsukruk, V. V. *Adv. Funct. Mater.* **2005**, *15*, 771.
(49) Nolte, A. J.; Rubner, M. F.; Cohen, R. E. *Macromolecules* **2005**, *38*, 5367.
(50) Stafford, C. M.; Harrison, C.; Beers, K. L.; Karim, A.; Amis, E. J.; VanLandingham, M. R.; Kim, H.-C.; Volksen, W.; Miller, R. D.; Simonyi, E. E. *Nat. Mater.* **2004**, *3*, 545.
(51) Gunawidjaja, R.; Jiang, C.; Ko, H.; Tsukruk, V. V. *Adv. Mater.* **2006**, *18*, 2895.
(52) Jiang, C.; Rybak, B. M.; Markutsya, S.; Klatidis, P. E.; Tsukruk, V. V. *Appl. Phys. Lett.* **2005**, *86*, 121912.

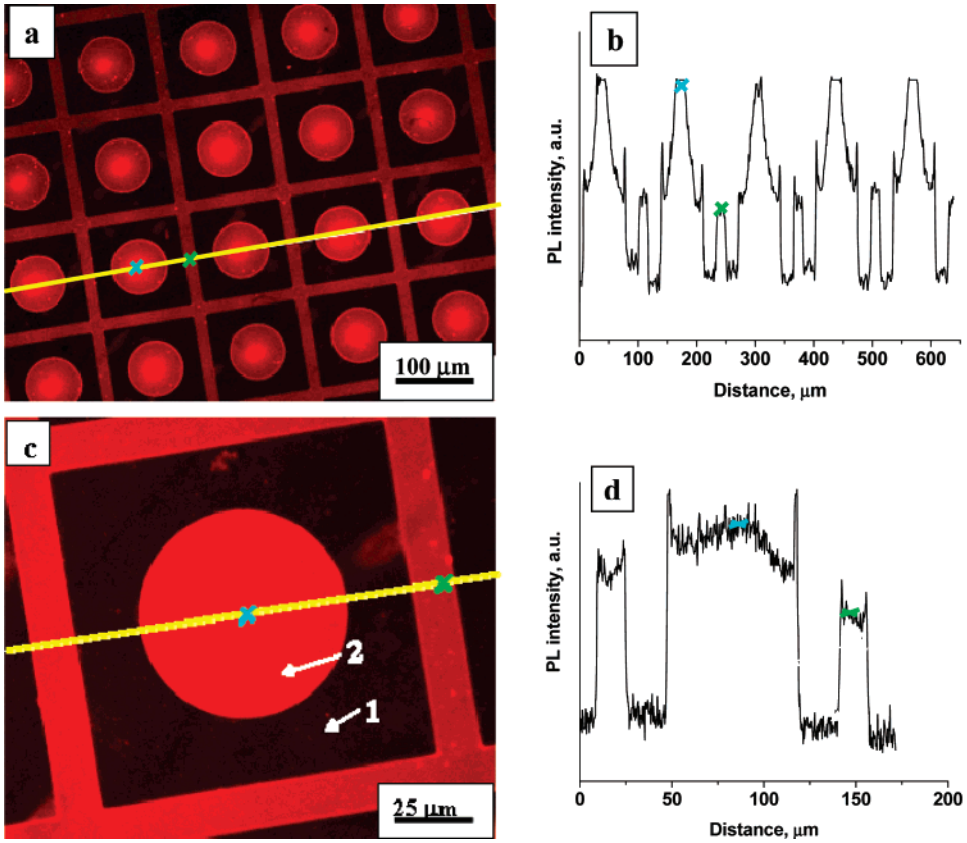

Figure 7. Fluorescent images of the QD film picked up on microfabricated silicon wafer with microscopic cavities at different magnifications (a, c). (b, d) plots of the PL intensity across the yellow lines on parts a and c, respectively. Central QD layer was deposited using 0.1% solution.

does not affect their optical response (Figure 6). The intensity of the PL peak is directly proportional to the number of QD nanoparticles within the LbL films which is expected for a low concentration of nanoparticles when they do not aggregate (Figure 6).[15] However, the overall PL intensity of the LbL films deposited on various solid substrates is relatively low due to a low concentration of QD nanoparticles and probably due to the quenching effect from the solid substrate. This low intensity makes it very difficult to collect high quality fluorescence images and fast collection of emission spectra without overexposing the LbL fims.[24] Here, it worth noting that, under certain conditions, temporal (within hours) variation of PL intensity is observed and was discussed in detail in a separate publication.[53] However, all PL intensity data discussed here are collected under identical experimental conditions and thus can be compared directly.

The LbL-QD film on the microfabricated silicon substrate with microfabricated cavities showed a very interesting and unexpected distribution of the fluorescent intensity which followed the pattern of the microfabricated array (Figure 7). The regions of the LbL films not in direct contact with the silicon surface but suspended across openings showed a dramatic rise in the fluorescence intensity as compared to the dark areas of the films lying directly on the silicon. Bright circular areas correspond to fluorescence of LbL films covering the array of circular openings in the microfabricated silicon wafer. There is a regular variation of PL intensity with maximum intensity located in the center of the LbL films suspended across openings. The peak intensity exceeds manifold the PL intensity of the LbL film located onto the silicon surface (see the cross-section of the PL intensity in Figure 7b). The overall characteristics of the emission

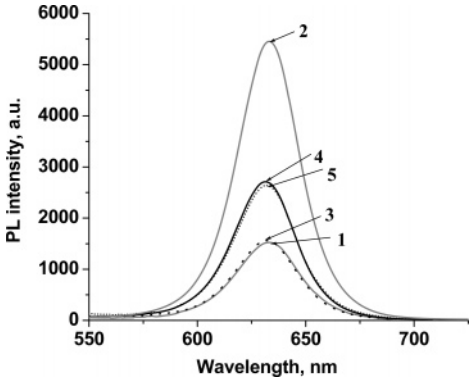

Figure 8. Emission spectra of the 9QD9 film in contact with the silicon (1), PDMS (3), and glass (5) surface and in free-standing state over cavity in silicon (2) and PDMS (4) substrate. Spectra 1 and 2 correspond to locations shown by arrows in Figure 7c. Central QD layer was deposited using 0.1% solution.

spectra of LbL films are very similar as demonstrated for two selected locations (1 and 2 in Figure 7a) with an intensity about 4 times higher on a freely suspended region (Figure 8). Both position and half-width of a single emission peak are virtually identical for supported and suspended regions of the LbL film (Figure 8).

A less dramatic increase in the PL intensity was observed for LbL films with QDs deposited on PDMS substrates with similar microfabricated cavities (Figure 8). In this case, we have observed similar but weaker phenomenon of increasing PL intensity for LbL-QD films freely suspended across microscopic openings.

Apparently, the highly variable fluorescence intensity distribution is controlled by the underlying microfabricated silicon substrate. In the design exploited here, the LbL-QD film covers completely a piece of silicon wafer with the microfabricated

(53) Zimnitsky, D.; Jiang, C.; Xu, J.; Lin, Z.; Tsukruk, V. V. *Langmuir* **2007**, *23*, 4509.

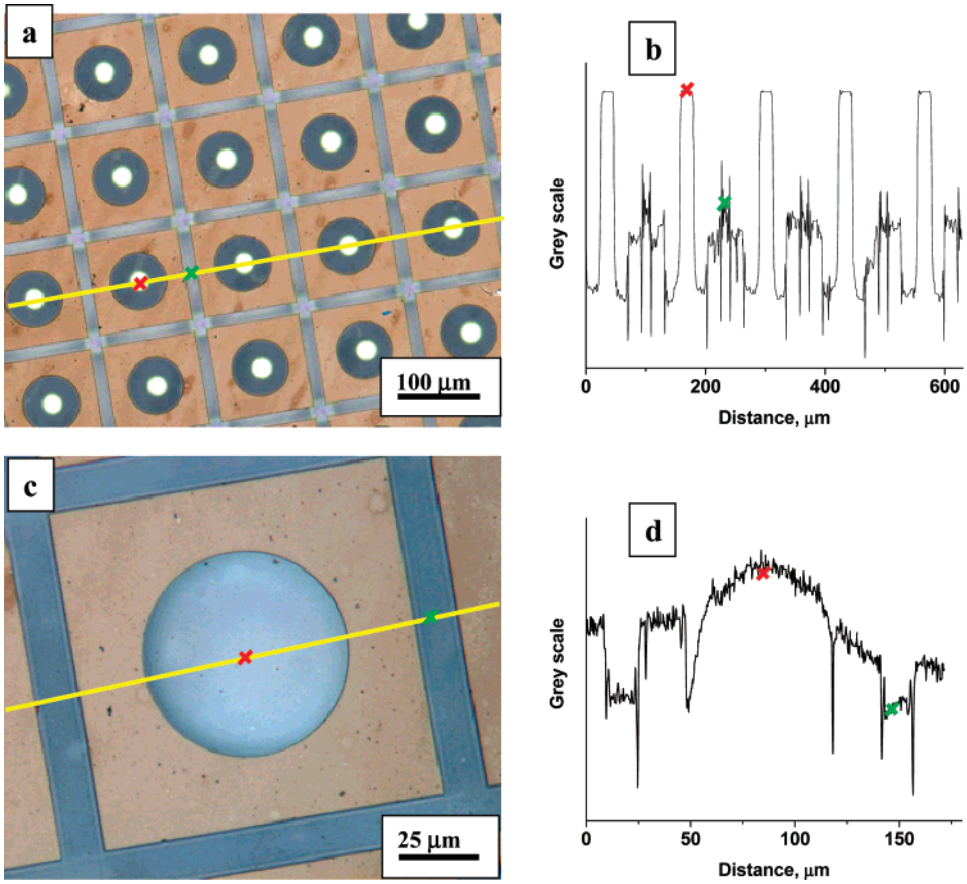

Figure 9. (a, c) Bright-field images of 9QD9 film picked up on the silicon surface with cavities at different magnification similar to those on the fluorescent images in Figure 7. (b, d) plots of brightness intensity across the lines on panels a and c, respectively.

array of optical cavities with a cylindrical shape (diameter 70 μm, depth 80 μm) separated by narrow trenches of the same depth as described in detail in our recent publication.[54] These cavities served for the enhancement of the light reflection for photothermal imaging array.

We suggest two major factors affecting the PL intensity for the same film in contact with the substrate surface and freely suspended over microscopic surfaces. These are the quenching of PL by the surface and the increase of intensity due to highly reflective material on the bottom of the cavity which creates backlight conditions. Since PDMS is nonreflective, the PL intensity of the film freely suspended over cavities in PDMS can be considered not affected by surface and optical effects (Figure 8, curve 4). The PL intensity for the LbL-QD film in contact with silicon and PDMS surfaces is comparable and lower than that freely suspended over cavities in PDMS. This decrease can be related to the quenching of the PL caused by its proximity to the silicon surface.[55−57] This lower emission can be caused by the nonspecific energy transfer between QDs and the surface which might efficiently quench the light-emission despite relatively large distance to the substrate surface. It was reported that quenching of QD photoluminescence is still pronounced on the distance from the surface as high as 30 nm and even more.[55,56]

The PL intensity of the same film transferred on glass is comparable with those for the films freely suspended over PDMS cavities. This can be expected because glass is highly transparent and the quenching effect is negligible.

The characteristic bright circles in the center of microcavities, which can be seen on bright-field images at lower magnification (Figure 9a) are related to the illumination of the microscopic cavities by a larger light source located directly above the cavity. A bright-field image at higher magnification shows that if the light source is closer to substrate surface the reflected intensity becomes more uniform but still with the highest intensity in the center (Figure 9c). Profiles for the reflected light at both magnifications are similar to profiles for the fluorescent intensity with a minor difference related to higher reflected intensity around the circular cavity (compare Figures 7d and 9d). In fact, the optical cavity array with LbL film shows a very similar appearance in a bright-field mode (see two different images at identical magnifications in Figures 7 and 9).

The PL intensity for a film freely suspended over cavities in the silicon substrate is approximately two times higher than the intensity of a free-standing film over cavities in PDMS. It can be related to the reflection of an incident light from a highly reflective bottom of the silicon cavities as illustrated in Figure 10. In this schematic, we illustrate light reflection for the film in direct contact with the substrate as compared to those in the free-suspended state (Figure 10a,b). In the latter case the additional excitation is possible by reflected light, which along with the suppression of the quenching effect should cause enhanced light-emission. Moreover, the cylindrical shape of the cavities should result in nonuniform distribution of the reflected light with the

(54) Jiang, C.; McConney, M. E.; Singamaneni, S.; Merrick, E.; Chen, Y.; Zhao, J.; Zhang, L.; Tsukruk, V. V. *Chem. Mater.* **2006**, *18*, 2632.
(55) Duijs, E. F.; Findeis, F.; Deutschmann, R. A.; Bichler, M.; Zrenner, A.; Abstreiter, G.; Adlkofer, K.; Tanaka, M.; Sackmann, E. *Phys. Status Solidi B* **2001**, *224*, 871.
(56) Wang, C. F.; Badolato, A.; Wilson-Rae, I.; Petroff, P. M.; Hu, E. *Appl. Phys. Lett.* **2004**, *85*, 3423.
(57) Curutchet, C.; Cammi, R.; Mennucci, B.; Corni, S. *J. Chem. Phys.* **2006**, *125*, 054710.

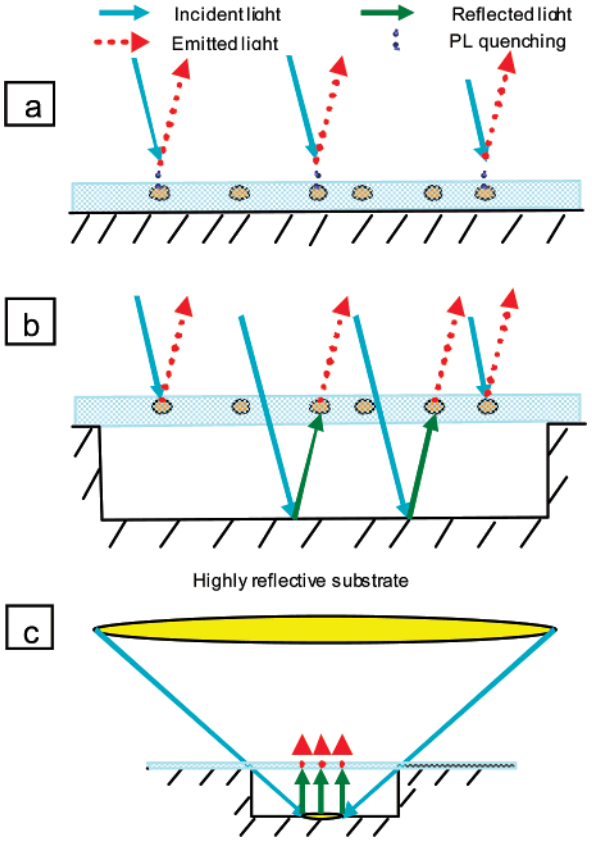

Figure 10. (a) Schematic of light reflection and quenching for QDs-LbL film in close proximity to the surface. (b) Illustration of the emission enhancement caused by the reflection of incident light from highly reflective bottom of the cavity. (c) Illustration of light focusing effect resulting in bright circles in the center of the cavities (see bright-field and fluorescent images in Figures 7c and 9c).

highest intensity in the center, thus, further enhancing the film emission from the central region as indeed observed in experiments (Figure 10c). We should take into account that surface coverage of QDs in the monolayer is as low as 6%, and the incident light almost completely goes through the free-standing film and reflects from the highly reflective bottom of the cavities. As a result, the overall intensity of excitation light for free-standing locations of the film over cavities in silicon is higher compared with films freely suspended over the nonreflective PDMS substrate (Figure 8, curves 2 and 4). The overall reflection is crucially dependent on the geometry of the cavity and the distance between the light source and the substrate. This allows us to control enhanced light-emission designing the shape and reflective properties of cavities and adjusting distance between light source and QDs-LbL film.

Conclusions

In conclusion, we have demonstrated that the QD monolayer with low density of nanoparticles can be efficiently encapsulated into flexible, free-standing, nanoscale (thickness below 60 nm) films. These LbL-QD films are stable in acetone and water and are mechanically robust to sustain transfer onto various substrates, high residual stresses, and multiple deformations and show modest light-emission intensity. A dramatic (manifold) increase in PL intensity was discovered for LbL-QD nanoscale films lifted from solid substrates and suspended across cylindrical optical cavities onto the microfabricated silicon substrate. This phenomenon is related to the peculiar enhancement of the light reflection at the microfabricated cavities as well as to the elimination of the surface quenching contribution after lifting. The effect of the enhanced fluorescence observed here can be promising for the development of efficient QD-containing and flexible nanoscale polymeric films which can be employed in fluorescence-based sensing devices operating in the reflection mode with much enhanced light-emission intensity in comparison with regular QDs tethered to or embedded in surface layers on solid substrates. We suggest that by optimizing the light reflective properties of the microfabricated substrate via design of microcavities it might be possible to tune and greatly enhance the PL intensity of QDs encapsulated in the free-standing LbL films thus greatly improving sensitivity of flexible organic electronic devices with encapsulated QDs.

Acknowledgment. This work was supported by the AFOSR, FA9550-05-1-0209 and NSF−CTS-0506832 Grants, and the 3M Non-tenured Faculty Award (Z.L.). J.X. thanks the Institute for Physical Research and Technology of Iowa State University for a Catron graduate research fellowship. We also thank Maryna Ornatska for technical assistance.

LA7014644